Attenuation-Emission Alignment in Cardiac PET/CT with Consistency Conditions

Adam Alessio, *Member, IEEE*, James Caldwell, Grace Chen, Kelley Branch, Paul Kinahan, *Senior Member, IEEE*

***Abstract*— Misaligned attenuation correction factors lead to artifacts and quantitative errors in cardiac PET images, potentially resulting in inaccurate interpretation and/or incorrect clinical decisions. Artifacts from misaligned attenuation-emission scans are common with conventional PET imaging. The potential for misalignment/artifacts is further increased in dual modality PET/CT systems since CT images a snapshot of the respiratory cycle and PET images multiple respiratory cycles. In this work, we developed and tested a method for automated alignment of attenuation and emission data. The alignment process enforces the Radon consistency conditions on the emission data and is derived from previous work by Welch et al. The attenuation image volume is aligned through simple rigid body transformations with the emission data. We test the process with simulated data and measured patient data from two ammonia cardiac PET/CT exams.**

I. Introduction

The goal of this work is to improve the attenuation-emission alignment in cardiac PET/CT imaging. Misaligned attenuation correction factors lead to artifacts and quantitative errors in cardiac PET images, potentially resulting in inaccurate interpretation and/or incorrect clinical decisions. Artifacts from misaligned attenuation-emission scans are common with conventional PET imaging (21% of cardiac cases have artifacts from attenuation [5]). The potential for misalignment/artifacts is further increased in dual modality PET/CT systems since a CT scan images a snapshot of the respiratory cycle and a PET scan images multiple respiratory cycles [2]. In this work, we developed and tested a method for automated alignment of attenuation and emission data. The alignment process enforces the Radon consistency conditions on the emission data and is derived from previous work by Welch et al [8]. The optimal rigid body transformation of the attenuation image volume is found that results in the most consistent attenuation corrected emission data and improved attenuation-emission alignment. We test the process with simulated data and measured patient data from an ammonia cardiac PET/CT exam.

Manuscript for 2006 IEEE NSS/MIC proceedings received November 15, 2006. This work was supported by NIH grant CA74135 and CA115870.

A. Alessio, P. Kinahan, and J. Caldwell are with the Dept. of Radiology, University of Washington, Seattle, WA 98195 USA. (telephone: (206)543-2419, email: aalessio@u.washington.edu)

J. Caldwell is also with G. Chen and K. Branch in the Division of Cardiology, University of Washington, Seattle, WA 98195 USA

II. Alignment Metric

The attenuation image, formed from scaling the CT image volume to attenuation coefficients at PET energy[3], is aligned with the PET emission image by applying rigid body transformations until the attenuation corrected PET data minimize an alignment metric based on the two-dimensional Radon consistency conditions. In this work, we enforce the first three moments of the Helgason-Ludwig consistency conditions on 2-D Radon transforms in a method originally proposed by Welch et al. [8]. Their method uses Natter's formulation of the consistency conditions

$$\Phi_{m,k} = \int_0^{2\pi} \int_{-\infty}^{\infty} s^m e^{ik\phi} e^{A(s,\phi)} E(s,\phi) ds d\phi \qquad (1)$$

where $E(s,\phi)$ are the measured data, $A(s,\phi)$ are the projections of the attenuation image, $m \geq 0$ is the moment being computed, and k is Fourier component [6]. The radial distance from the center of rotation s and the azimuthal angle of rotation ϕ index the Radon transform space.

If the attenuation corrected projection data is consistent, $\Phi_{m,k} = 0$ when $k > m$ or when $k+m$ is odd. This relationship is a result of the fact that the moments of projections through an object are periodic in azimuthal angle. Figure 1 plots the projection moments (inner integral over s in (1)) for noise-free data versus azimuthal angle. The zero-order moment of the consistency conditions states the well known property that the sum of the projection data at one view of parallel-beam projections is a view-angle independent constant. The zeroth moment in figure 1 shows that the sum of projections is the same at all angles. The first order moment shows that the projections of the center of mass in the object (a single point) form in a sine wave with period one in the sinogram. The 2nd moment plot reveals a sine wave with period 2; the 3rd contains sine waves with periods 1 and 3. Likewise, higher order moments result in combinations of sine waves with greater periods. If projections are inconsistent, the moments will contain higher frequency information. The outer integral of (1) performs the Fourier transform of these moments; if the Fourier coefficients greater than the moment ($k > m$) have values, then the projections are inconsistent.

Bromiley and Welch, in a follow-up to their original work, used these conditions to perform attenuation-emission alignment in conventional PET imaging through transformations of

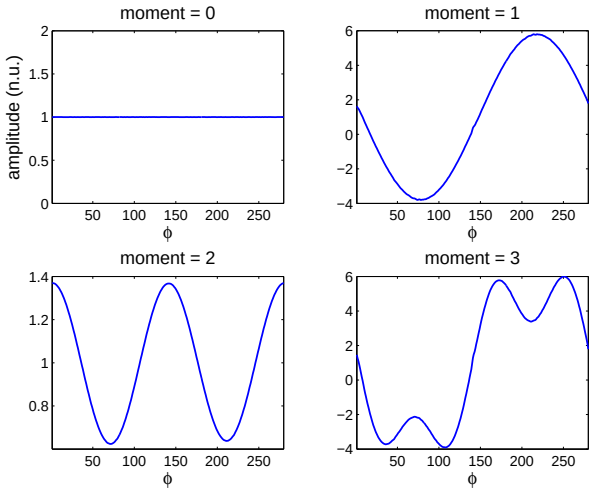

Fig. 1. Moments of noise-free projection data versus azimuthal angle reveal the periodicity of higher order moments and conceptually support the proposed formulation of the Radon consistency conditions. Curves are presented in normalized units.

a flawed (mis-aligned) attenuation image [1]. In this work, we modify their method for use with cardiac PET/CT imaging. We find the attenuation image which minimizes the objective function defined as:

$$\hat{\Phi} = \sum_{z} \sum_{m=0}^{3} \sum_{k=m+1}^{9} \Phi_{m,k}(z) \qquad (2)$$

where $\Phi_{m,k}(z)$ is calculated for each transaxial slice z.

III. Optimization Algorithm

The search for the optimally aligned attenuation map is performed with a simplex algorithm [4]. In our method, the algorithm is optimized over six rigid-body transformation variables: volume translations in x, y, z and rotations around the x, y, z axis. A single PET field of view (FOV) spans approximately 15cm in the z direction. In this work, we enforce the consistency conditions over the central 12cm (central slices) to enforce alignment in the problematic regions for cardiac imaging (mediastinum and right diaphragm) and to allow for errors at the edge of the axial FOV due as the attenuation image is translated and rotated out of the FOV. Furthermore, most mismatch of attenuation/emission images in PET/CT occurs because of respiratory motion which is primarily a z axis translation. We modified the simplex optimization to preferentially search the z translation space and allow for greater variation in z translation than the other variables. This customized approach attempts to avoid convergence to erroneous local minima.

IV. Methods

A. NCAT Simulations

We tested the alignment process with noise-free PET simulations of the NURBS-based Cardiac Torso (NCAT) phantom[7]. We generated emission data for full inspiration and full expiration of the respiratory cycle. We attempted to align the attenuation image from full inspiration with the emission data from full expiration. This is an example of a worse case alignment scenario.

B. Patient Studies

We tested the alignment process with two sets of patient data from N13-ammonia cardiac perfusion PET/CT studies. These studies were performed on a General Electric Healthcare (Waukesha, WI) DSTE PET/CT Scanner. The attenuation map and partially corrected projection data were extracted for offline processing. All image transformations and reconstructions were performed with custom software (not with the product reconstruction engine).

Patient A is a study with "correct" attenuation-emission alignment as deemed by visual inspection of attenuation and emission images. With this realistic noise study, we first evaluated the behavior of the objective function with multiple transformations. There are 6 transformation dimensions to explore; we tested the value of the objective function for various z-translations (our experience shows this is the dimension with greatest frequency of misalignment) and other transformation values. We forced a 16mm inferior translation on the attenuation map and evaluated the objective function using different orders of moments to assess the presence of local minimum. Secondly, we forced a arbitrary (x,y,z) translation = (-16.4,-10.9,19.6)mm and rotation around (x,y,z) axis = (3, 0, 1) degrees for the attenuation map. This misaligned map was the starting point for the simplex search for the optimal transformation.

Patient B is a study with initially misaligned attenuation and emission images. We performed the simplex search for 70 iterations to find an "aligned" attenuation map.

V. Results

A. NCAT Simulations

Figure 2 presents reconstructions (filtered backprojection with ramp filter) of these noise-free simulations. The proposed method improved the alignment of the emission and attenuation images. The simplex search determined the optimal transformation of the full-inspiration attenuation image to be (x,y,z) translation = (5.8,-1.9,-22.7)mm and rotation around (x,y,z) axis = (4.4, -1.7, 0.2) degrees.

The aligned attenuation image reduced several of the artifacts due to attenuation errors, particularly in the myocardium. It is important to note that the alignment will never be "perfect" because there is a non-rigid deformation between inspiration and expiration and we are only enforcing a rigid-body transformation. This worse case scenario highlights this reality showing that there are still major errors in the PET image with the aligned attenuation case. In practice, we assume that the attenuation image is relatively well-aligned with the emission data and simple rigid-body changes account for most of the mismatch errors. We acknowledge that this assumption is not accurate in some cases.

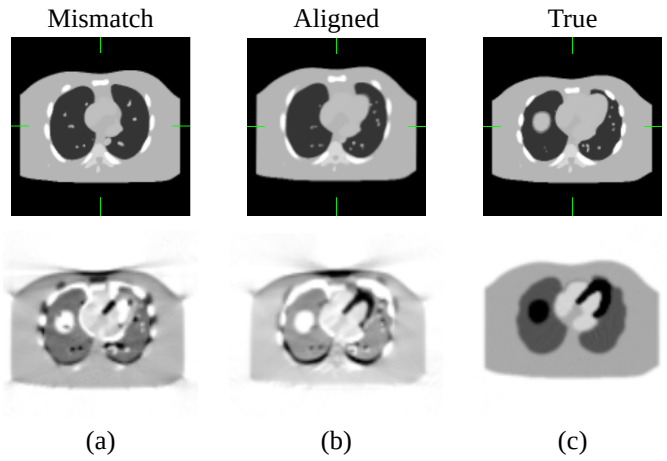

Fig. 2. Transaxial views of reconstructions of noise-free simulated PET data from the NCAT phantom. The PET images (row 2) were attenuation corrected with corresponding attenuation images from row 1. Column (a) used emission data from full-expiration and attenuation correction from full-inspiration, column (b) used emission data from full-expiration and the attenuation from full-inspiration aligned to the emission data with the proposed method, column (c) used emission and attenuation correction data both from full-expiration. The alignment process reduced the artifacts that are present in the AC PET images using a mismatched attenuation image.

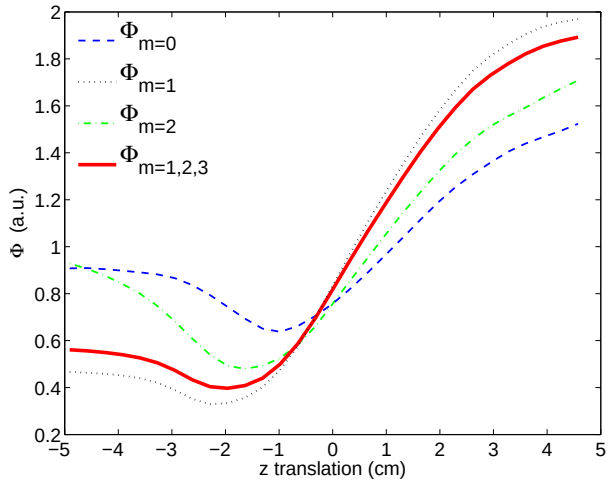

Fig. 3. Objective function values for patient A as a function of translation in axial location with the other transformation dimensions fixed. Plots the values of 2 for different moments and for the sum of moments $m = 0, 1, 2$. These curve shows that the objective function is well-behaved for this patient and for this dimension. The minimum should occur at approximately -1.6cm since we forced a translation of 1.6cm on the original "aligned" data.

B. Patient Studies

For patient A with a 16mm forced z translation, the value of $\hat{\Phi}$ as a function of z translation of the attenuation image is presented in figure 3. The value of the objective function across two transformation parameters, with the other parameters fixed, appears in figure 4. This offers some insight into the behavior of the objective function for a single patient, but does not take into account the effect of the other transformation dimensions. For this example, the objective function is well-behaved with no local minimum in the range of interest. The variation of slope as the minimum is approached from different directions points to the reality that the choice of initial values for the transformation will effect the speed of convergence for this application.

We also performed the full alignment optimization for patient A when the attenuation map was given a known misalignment. After 150 iterations of the simplex algorithm, the estimated alignment transformation was an (x,y,z) translation = (-21.8, -7.1, 25.7)mm and rotation around (x,y,z) axis = (-1.1, 1.5, -0.5) degrees. These values have a difference of (x,y,z) translation = (5.3,-3.8,-6.1)mm and rotation (x,y,z) = (1.8, 1.5, 0.5) degrees with the forced misalignment. Given the overall system resolution and noise levels in ammonia studies, these differences are low. Furthermore, assessment of the images in figure 5 prove that the automatically-aligned attenuation map reduces artifacts in the attenuation corrected PET image, particularly along inferior wall.

In patient B, the proposed method successfully realigned the attenuation image as presented in figure 6. Note the major artifacts in the emission image when using an mismatched attenuation image and the lack of these errors in the aligned image.

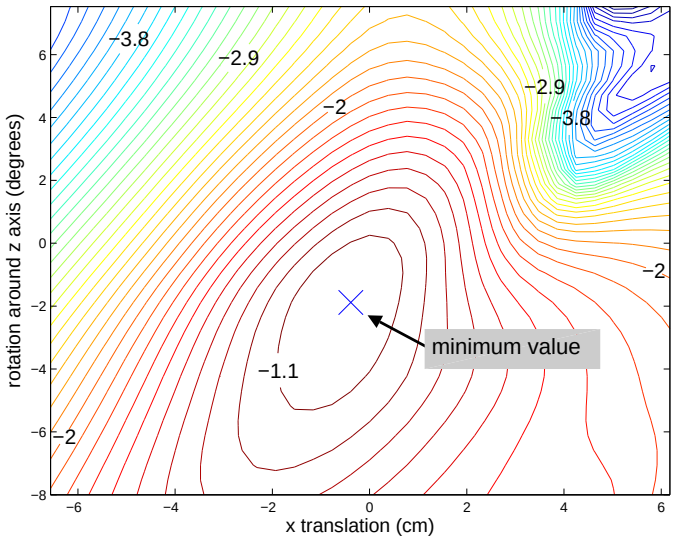

Fig. 4. Contour of objective function values for patient A as a function of rotation around z and translation in x with the other transformation dimensions fixed. This case started with original "aligned" data, the minimum should occur at approximately (0,0).

C. Algorithm Performance

The proposed alignment algorithm was not optimized. The steps for each evaluation of the objective function include 1) transform the attenuation volume, 2) forward project, 3) compute moments, 4) FFT the moments in ϕ, 5) compute the objective function value. In the clinical patient studies presented here using 8×10^5 image voxels and a projection space with 4×10^6 entries, each function evaluation took 3 seconds on a 2.3GHz PowerPC G5. A total optimization with 150 simplex iterations required 15 minutes.

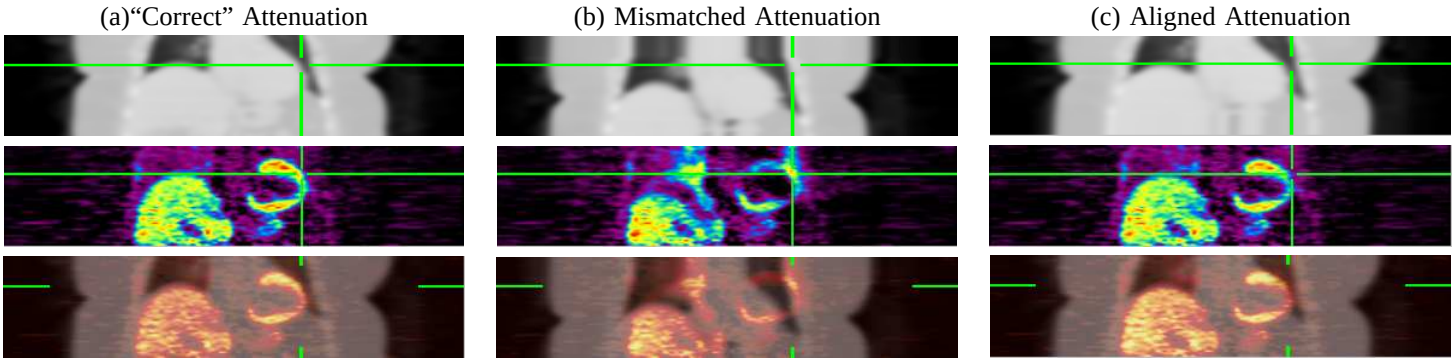

Fig. 5. Coronal views of a cardiac ammonia PET/CT study from patient A. The PET images (row 2) were attenuation corrected with corresponding attenuation images from row 1. The original CT scan provided reasonable attenuation correction as deemed by visual inspection and is labeled “correct” (a). We shifted the attenuation image to force a mismatch (column b). The alignment process successfully aligned the attenuation image (column c) with the emission data. Note that in column (b) the PET myocardium appears in the CT lung space and chest wall leading to artifacts throughout the lateral wall in the PET image.

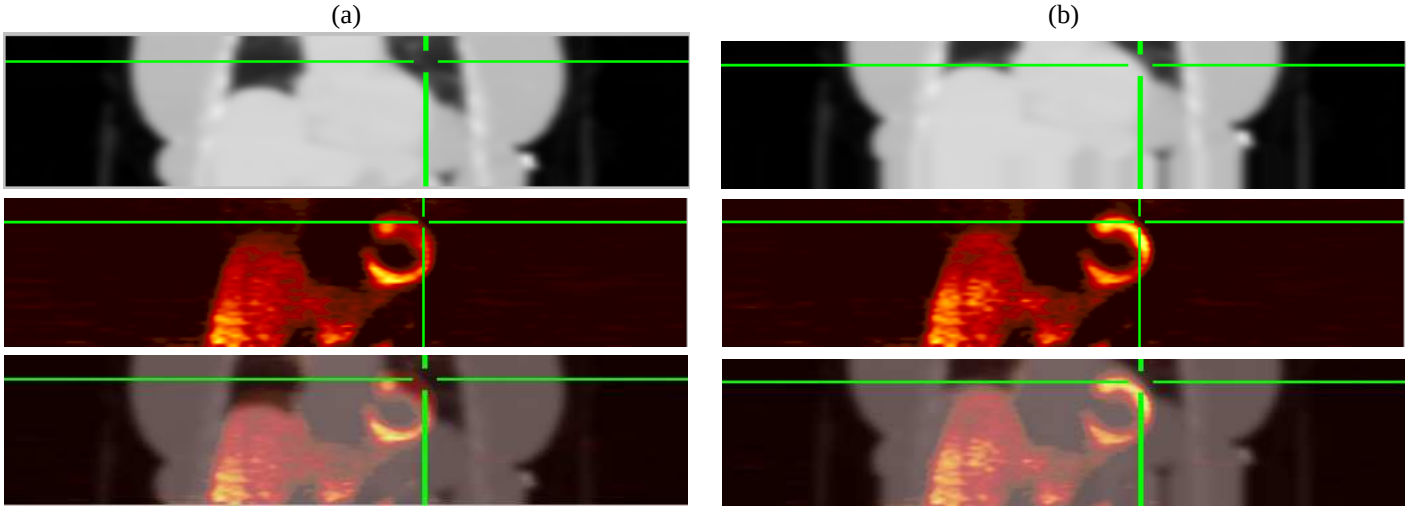

Fig. 6. Coronal views of reconstructed images from Patient B ammonia PET/CT study. Column (a) presents the original attenuation map (row 1), attenuation corrected PET image (row 2), and fused PET/CT image. Column (b) presents the images after alignment with the proposed method. The alignment process reduced the incorrect attenuation correction values along the lateral free wall, removing the artifactual perfusion defect in the PET image.

VI. Conclusion

We developed an automated attenuation correction alignment method for use with cardiac PET/CT imaging. We demonstrated the efficacy of the proposed method with simulation studies and measured patient data. Initial evaluation of this optimization algorithm shows that it converges to transformation values at a global minimum leading to improved attenuation correction for cardiac PET imaging. The current implementation of the algorithm is fairly slow requiring 70+ iterations for typical whole-body patient noise levels and data sizes. We intend to explore faster gradient based optimization algorithms and to speed the objective function calculation through the use of only subsets of the emission data at each function evaluation. A faster, gradient based approach will allow us to explore more realistic non-rigid deformations of the attenuation map for potentially improved alignment.

References

[1] A. Bromiley, A. Welch, F. Chilcott, and et al. Attenuation correction in PET using consistency conditions and a three-dimensional template. *Nuclear Science, IEEE Transactions on*, 48(4):1371–1377, 2001.

[2] GW Goerres, C Burger, E Kamel, and et al. Respiration-induced attenuation artifact at PET/CT: Technical considerations. *Radiology*, 226(3):906–910, 2003.

[3] Paul E. Kinahan, Bruce H. Hasegawa, and Thomas Beyer. X-ray-based attenuation correction for positron emission tomography/computed tomography scanners. *Semin Nucl Med*, 33(3):166–179, 2003.

[4] J.C. Lagarias, J. A. Reeds, M. H. Wright, and P. E. Wright. Convergence properties of the Nelder-Mead simplex method in low dimensions. *SIAM Journal of Optimization*, 9(1):112–147, 1998.

[5] C Loghin, S Sdringola, and KL Gould. Common artifacts in PET myocardial perfusion images due to attenuation-emission misregistration: Clinical significance, causes, and solutions. *J Nucl Med*, 45(6):1029–1039, 2004.

[6] F. Natterer. *The Mathematics of Computerized Tomography*. Wiley, New York, 1986.

[7] W.P. Segars and B.M.W. Tsui. Study of the efficacy of respiratory gating in myocardial SPECT using the new 4-D NCAT phantom. *Nuclear Science, IEEE Transactions on*, 49(3):675–679, 2002.

[8] A. Welch, C. Campbell, R. Clackdoyle, and et al. Attenuation correction in PET using consistency information. *Nuclear Science, IEEE Transactions on*, 45(6):3134–3141, 1998.